Value Distribution Strategies for Hydrothermal and EGS Resource Estimation in Geothermal Exploration

R. Chadwick Holmes and Jozina B. Dirkzwager

Chevron Corporation, Houston, TX 77002

chadwick.holmes@chevron.com, jozina@chevron.com

ABSTRACT

For decades, the Volumetric Heat-in-Place (HIP) method has served as the preferred method for estimating recoverable heat and electrical power generation capacity in geothermal projects. Calculating probabilistic HIP assessments is a well-established practice using Monte Carlo simulations. However, important considerations remain in selecting the appropriate HIP derivation and accurately characterizing input distribution shapes and value constraints. This study re-examines HIP methodologies to address complexities and potential biases that may influence results. Using a simple Python codebase, probabilistic estimates of stored heat and electrical power are made with different HIP formulations. Results indicate fluid and steam contributions to stored heat are minor, but input distribution choices can significantly affect estimates. Lognormal distributions are recommended to mitigate certainty bias for subsurface parameters, focusing on reservoir area, thickness, and temperature. Sensitivity analysis reinforces the importance of selecting reasonable efficiency and recovery factors for accurate resource assessment. Real-world examples illustrate the methods in action for both hydrothermal and Enhanced Geothermal Systems (EGS), offering guidance on generating calibrated estimate ranges for consistent exploration assessments. When combined with an explorer's mindset and basic statistical checks for bias, the HIP method can provide both consistency and value to a geothermal exploration program.

1. INTRODUCTION

The Volumetric Heat-in-Place (HIP) method was introduced in USGS Circular 726 as part of a comprehensive nationwide geothermal resource assessment for the United States (Nathenson and Muffler, 1975). It aimed to address earlier estimates that sometimes differed by orders of magnitude (White and Williams, 1975). The approach focused on "stored heat," i.e., thermal energy exceeding surface conditions within the upper crust. Equation 1 defined the stored heat in the reservoir, and Equation 2 related reservoir heat to potential electrical power generation capacity:

$$q_R = (A\,h)(\rho_r c_r)(T_R - T_0), \tag{1}$$

$$MW_e = e_{conv}\, R\, q_R \left(\frac{1}{PL}\right), \tag{2}$$

where A, h, $\rho_r c_r$, T_R, and T_0 are the area, thickness, volumetric specific heat, temperature, and reference temperature for the reservoir, respectively. The U.S. mean annual surface temperature of 15°C was used for the reservoir reference temperature. Power plant capacity factor (P) and operational life of the field (L) are not explicitly described by Nathenson and Muffler (1975), although estimates in Circular 726 are time-based, provided in both MWe-centuries and MWe-30 years. These factors are noted here for consistency with later publications (e.g., Sarmiento et al., 2013; Quinao and Zarrouk, 2014, Ciriaco et al., 2020). Additionally, a 25% recovery factor (R) was applied under the assumption that half the reservoir volume could be accessed by fluids and half of the heat in that sub-volume could be recovered at the wellhead. The conversion efficiency (e_{conv}) was related to reservoir temperature and ranged from 8-12% for hot water systems (see Table 15, Nathenson and Muffler, 1975).

Four years later, USGS Circular 790 revised the HIP governing equations while updating the national resource estimate (Brook et al., 1979). Specifically, Equation 2 was replaced with a new calculation of MW_e linked to the concept of exergy or the maximum amount of work that can be produced from an energy system. First, the mass of fluid produced at the wellhead was calculated by Equation 3:

$$m_{wh} = \frac{R\, q_R}{(h_{wh} - h_f)}, \tag{3}$$

where h_{wh}, and h_f are fluid enthalpies at the wellhead and final state/rejection temperature of the power cycle. Next, electrical power generation capacity was derived from the maximum available thermodynamic work for the produced fluid (W_A), discounted by a utilization efficiency factor (e_{util}):

$$MW_e = e_{util}\, W_A \left(\frac{1}{PL}\right)$$

$$= e_{util} \left[m_{wh} \left(h_{wh} - h_f - T_{fK}(s_{wh} - s_f) \right) \right] \left(\frac{1}{PL} \right), \tag{4}$$

where T_{fK} is the power cycle reference temperature or final state temperature (in Kelvin), s_{wh} is fluid entropy at the wellhead, and s_f is fluid entropy at T_{fK}. Here, we've again added the field operational lifespan terms (PL) for consistency in characterizing MW_e. Circular 790 also used Monte Carlo methods with input variable distributions to estimate probabilistic heat in place and power generation capacity. This update has been widely adopted ever since; however, it requires careful choices regarding distribution shapes and bounds.

Note that the efficiency terms in Equations 2 and 4 differ; whole-system geothermal conversion efficiency is around 10%, based on empirical data, and has been modeled as a function of both reservoir temperature and enthalpy (e.g., Zarrouk and Moon, 2014; Ciriaco et al., 2020). Utilization efficiency relates to mechanical and other losses in the power cycle, ties to the power plant design, and has typical reported ranges of 40-50% (Brook et al., 1975; Quinao and Zarrouk, 2014). Reference temperatures also differ. The reservoir reference temperature defines a general baseline for stored heat calculations, sometimes linked to annual average surface conditions (Nathenson and Muffler, 1975), power plant rejection temperature (Ciriaco et al., 2020), or the triple-point temperature for water (Takahashi and Yoshida, 2016). By contrast, the final state temperature generally relates to measurements within the power plant, e.g., the saturation temperature at the separation pressure for a single flash plant, or the pinch point temperature for binary plants (Garg and Combs, 2015).

Adding more complexity, total stored heat in the reservoir can be divided into components from the rock and the water within its pore space (e.g., Muffler and Cataldi, 1978). Additionally, heat from water can be split into liquid and steam components (e.g., AGEA, 2010):

$$q_R = q_{rock} + q_{liquid} + q_{steam}$$
$$= [\rho_r c_r (1 - \varphi)(T_R - T_0)] + [\rho_{wR}\varphi S_w(h_{wR} - h_f)] + [\rho_{sR}\varphi(1 - S_w)(h_{sR} - h_{wR})], \tag{5}$$

where ρ_{wR} and ρ_{sR} are the density of water and steam at reservoir temperature, φ is porosity, S_w is water saturation, and h_{wR} and h_{sR} are liquid water and steam enthalpies at reservoir temperature.

Although 50 years have passed, the USGS HIP estimation model still uses a combination of these equations to define stored heat and electrical power generation capacity. However, the HIP input values and equations have been frequently adjusted by various authors. Table 1 shows examples of this evolution over time.

Table 1: Selected studies addressing geothermal resource estimation by the HIP method. Study-recommended equations and variable assignments are noted to highlight the variety of interpretations.

Study	Recommended Equations	Ref. Temperatures	Recovery Factor	Efficiencies	Novelty
Williams, 2004, 2008	q_R: (1) MWe: (4)	$T_0 = 15°C$	8-20% (fracture dominated), 10-25% (sedimentary)	e_{util} = 0-40%	R tied to fracture models, e_{util} defined as a $f(T_R)$
Sanyal and Sarmiento, 2005	q_R: (5) MWe: (2)	T_f = 30°C	5-20% (liquid), 30-70% (steam)	e_{conv} = 47.7%	Alternate equation for steam fields
Tester et al., 2006	q_R: (1) MWe: (2)	$T_0 = T_R - 10°C$	2%, 20%	e_{conv} = 11-22%	EGS system focus, added factor for land accessibility
Garg and Combs, 2010	q_R: (5) MWe: (4)	$T_0 = T_f = 40°C$	0-20%	e_{util} = 45%	Inclusion of 0% lower end to R
Sarmiento et al., 2013	q_R: (5) MWe: (2)	$T_0 = T_f = 130°C$ (binary), 180°C (flash)	0-20%	$e_{conv} \approx$ 7-16%	R related to porosity, e_{util} defined as a $f(T_R)$
Zarrouk and Simiyu, 2013	q_R: (1) MWe: (2)	$T_0 = T_f = 170-180°C$ (flash)	8-30%, tiered by T_R, φ, fluid phases	e_{conv} = 12%	Added heat flow to Eq. 2; R is $f(h, \varphi)$, L = 50-100 years
Quinao and Zarrouk, 2014	q_R: (5) MWe: (2)	$T_0 = 175.35°C$ (flash) T_f = 15°C	17.5-20%	e_{conv} = 10-12%	Compared multiple methods using an effective efficiency
Garg and Combs, 2015	q_R: (5) MWe: (4)*	$T_0 = 15°C$, T_f = 105.36°C (binary), 151.831°C (flash)	0-20%	$e_{util} \leq 40\%$, should tie to T_R and T_f	*Authors prefer new W_A derivations for binary/flash
Takahashi and Yoshida, 2018	q_R: (1) MWe: (4)	$T_0 = T_f = 180°C$	13-30% (liquid-dominated)	e_{util} = 40%	R defined as a $f(T_R)$ for different T_0's

Interestingly, one of the stated purposes behind the publication of Circular 726 was to address the diversity of alternative approaches to resource estimation and establish a standardized HIP methodology (White and Williams, 1975). Once again, we find a multitude of options for generating geothermal resource estimates, potentially creating more confusion than confidence for an explorer seeking to measure the size of new opportunities.

Explorers must also consider the impact of human nature on resource estimation; several fundamental biases need to be addressed to ensure greenfield assessments remain both accurate and objective. First is overconfidence bias, which can be linked to exploration practice where innovation and creativity, essential traits for successful explorers, may lead to overestimating the size and chance of success of new prospects (Rose, 2001; Rose et al., 2004). Additionally, anchoring bias may cause explorers to highlight the upside potential and minimize downside risks when using successful analog fields to define prospect characteristics (Otis and Haryott, 2006). Parameter selection might introduce availability bias and confirmation bias, where explorers rely more heavily on readily available information and favor data that confirms existing beliefs, respectively. These biases can lead to inadequate calibration of estimates, with the effect of artificially reducing uncertainty in resource assessments (Otis and Haryott, 2010). Selecting appropriate distributions for each input variable, defining suitable value ranges, and testing for bias using statistical techniques (e.g., P90/P10 ratios) are essential steps in generating reasonable estimates of geothermal opportunities using the HIP method.

2. METHODS

This study addresses the challenges noted above by demonstrating conceptual trade-offs with field data from literature. Simulation code was constructed in Python for creating distributions, calculating stored heat and power generation estimates with Equations 1-5, and conducting sensitivity and comparative analysis. The fundamental topics of inquiry addressed by this work include:

    i.   Variation in stored heat estimates from different HIP method formulations
    ii.   Distribution choices and assumptions implicit in their construction
    iii.   Selecting appropriate reference temperatures, efficiencies, and recovery factors for different fields
    iv.   Maintaining an optimistic but bias-aware "explorer's mindset" for greenfield geothermal resource estimation

Field cases used for analysis come from previous publications, covering hydrothermal and EGS development concepts in different geothermal environments (Table 2).

Table 2: Field examples from literature used for comparing resource estimation methods.

Field Name	Sumikawa, Japan	Silver Peak, USA	Soulz-sous-Forêts, France
Geothermal System Type	Volcanic Arc, Hydrothermal	Fault-Based, Hydrothermal	Enhanced Geothermal System
Reservoir Area (km^2)	Low: 3, Mid: 4, High: 5	Low: 5.4, Mid: 11.1, High: 16.8	Low: 2, Mid: 3, High: 4
Reservoir Thickness (m)	Low: 1000, High: 2000	Low: 762, Mid: 1067, High: 1676	Low: 500, Mid: 1000, High: 1500
Reservoir Temperature (°C)	Low: 260, Mid: 290, High: 320	Low: 154, Mid: 174, High: 227	Low: 150, Mid: 180, High: 200
Rock Volumetric Specific Heat (kJ/m^3-K)	Low/Mid/High: 2700	Low/Mid/High: 2700	Low/Mid/High: 2700
Reservoir Porosity (%)	Low: 0, Mid: 2, High: 5	Low: 3, High: 7	Low/Mid/High: 1%
Water Saturation (%)	100%	100%	100%
Reference	Garg and Combs, 2015	GeothermEx, 2004; Garg and Combs, 2010	Hackstein and Madlener, 2021 (mid values)

3. RESULTS

3.1 Choice of USGS Method

Each review of the HIP method suggests modifications and additions (Table 1), similar to building renovations as occupants change over time. Applying the methodology now requires specification of which variant has been adopted, and one might question whether selecting the latest version significantly impacts the quality of a resource assessment. We approached this question by calculating six estimates of stored heat and power generation capacity for the same field. The first three use the 1975 form of the method (Equation 2), first with a single reservoir component (Equation 1), then introducing reservoir rock and fluid, and finally adding a steam component (Equation 5) through the addition of porosity and water saturation factors. The second group of three estimates follow suit, applying the 1979 USGS

calculations (Equations 3-4) along with different variations in the characterization of the reservoir. For this exercise, we referred to the parameterization of the Sumikawa geothermal field in Table 2, focusing on the mid values only to compare deterministic outcomes before introducing more complexity with a probabilistic assessment. While actual water saturation is around 1.0 for the Sumikawa field, we use $S_w = 0.5$ to demonstrate the impact of including reservoir steam in the estimate. Inputs not shown in Table 2 follow the constant or mid-range values from the source reference: $\rho_r c_r = 2700$ kJ/m^3-K, $R = 14\%$, $T_0 = 151.831°C$, $T_f = 15°C$, $e_{conv} = 12\%$, $e_{util} = 40\%$, $P = 95\%$, $L = 30$ years (Case 3, Garg and Combs, 2015).

Results of the individual component and total stored heat (thermal energy) values are shown in Figure 1. On first glance, the impact of including fluid and steam calculations in the total stored heat calculation appears trivial. At Sumikawa, porosity is estimated to be low (2%), at least partly explaining the minimal contributions of q_w and q_s in the 1975 and 1979 calculations with φ and S_w. Other authors have noted stored heat components for water tend to be an order of magnitude smaller than that for rock, and they account for ≤ 10% of the total thermal energy produced from the reservoir (Sanyal and Sarmiento, 2005; Quinao and Zarrouk, 2014). Although the Australian Geothermal Code requires rock, water, and steam factors for booking purposes (AGEA, 2010), one could argue that average porosity and water saturation are not well understood in early exploration and focusing just on the reservoir rock gives an appropriate first-order result (Ciriaco et al., 2020). Figure 1 supports that simplification.

The second important observation is the introduction of power cycle formulations (Equations 3-4) only slightly boosts the final power generation capacity estimate for Sumikawa field compared to the 1975 method values. All six calculations result in forecasts between 42-44 MWe for electrical power production, which matches the reported Sumikawa running capacity from 2010 (46 MWe) to a surprising degree (Sugino and Akeno, 2010). With such small differences in the outcome of all six calculations, putting greater effort into defining the input parameters well and applying the simplest (i.e., 1975) formulation seems most appropriate for early exploration applications of the HIP method. Additionally, because exploration resource estimates will typically not have this degree of accuracy, use of probabilistic simulation is highly recommended over generating single deterministic results as shown in Figure 1.
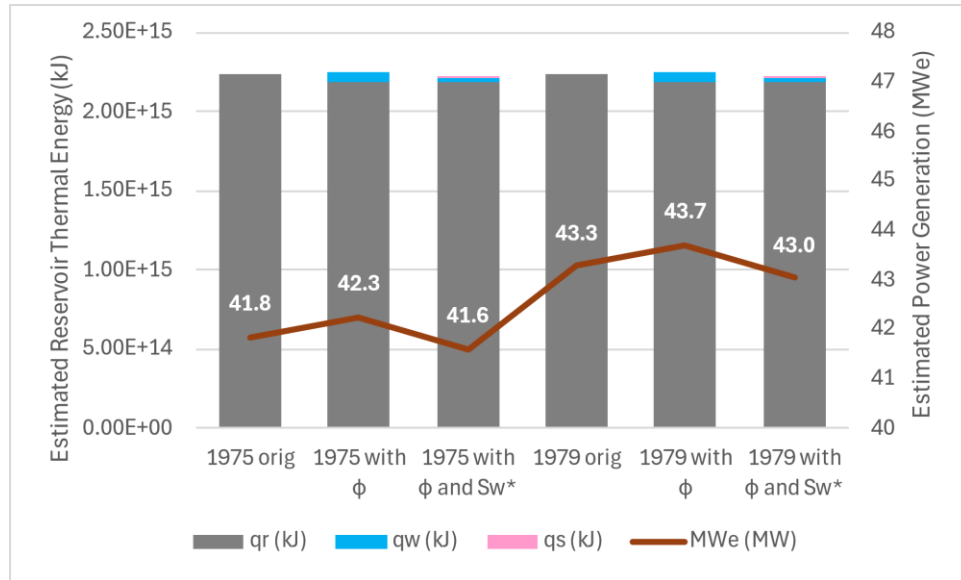

Figure 1: Estimates of total thermal energy in the reservoir and electrical power generation capacity at the Sumikawa geothermal field, calculated six ways. The stacked bars illustrate the total stored heat separated out into rock, water, and steam components whenever the equations used support differentiation. Annotated values and the line plot track the power generation estimate, also shown on the secondary y-axis.

3.2 Distribution Considerations

Imagine working on a resource assessment where reservoir temperature values determined from field data define a value range of 154 – 227°C, as noted for Silver Peak, NV in Table 2. If a uniform distribution is selected to represent reservoir temperature, running 1 million random samples on that distribution would result in a sample population like Figure 2A, where the 10%, 50%, and 90% probability (also referred to as P10, P50, and P90) values correspond to 161°C, 191°C, and 220°C, respectively. The mean matches the P50 value. The P90/P10 ratio, a proxy for variable uncertainty, is 1.36.

Triangular distributions are often used for geothermal resource assessments to focus greater probability on a "most likely" value and taper the probability of sampling values at the low and high extremes. Like the uniform distribution, the extremes are treated as hard cut-offs. Figure 2B illustrates a triangular distribution using the Silver Peak. The peak of the triangle defines the mode and is set by the mid-case value. Importantly, the P50 is a consequence of the distribution shape and not an input. The range defined by the P10, P50, and P90 values is narrower than for a uniform distribution, at 166°C, 183°C, and 207°C. The mean (185°C) is higher than the P50 due to a longer tail on the high side. A P90/P10 of 1.25 suggests that using a triangular distribution implies more certainty in the variable value than a uniform distribution.

Random variables representing natural properties of the earth tend to follow lognormal distributions (Rose, 2001), including geothermal reservoir area and temperature (Wilmarth et al., 2021). A key consideration when constructing these distributions is determining which percentiles should correspond to the low and high values, especially since lognormal distributions lack strict cut-offs at the extremes. Figure 2C shows Silver Peak reservoir temperatures sampled from a lognormal distribution constructed with the low and high values mapped to the P10 and P90. Note that the resulting percentiles can be an imprecise match because of the mathematical model that the distribution follows. For this example, the constructed distribution results in P10, P50, and P90 values of 148°C, 180°C, and 218°C. The sample mean is 182°C, and the P10/P90 is 1.47. Watching the extremes, the sample 1% and 99% percentiles are 126°C and 255°C, both outside of the original low/high bounds of the inputs. Using a lognormal distribution will thus introduce a broader range of potential outcomes than uniform or triangular distributions.

A truncated lognormal distribution is introduced in Figure 2D, where the cut-off end points correspond to the P01 and P99 values of the original lognormal. The resulting distribution concentrates higher probability of sampling across the rest of the distribution (demonstrated in Figure 2F), and the percentiles narrow accordingly. In this case, sampling the distribution leads to P10, P50, and P90 values of 149°C, 180°C, and 217°C, which is similar to the untruncated lognormal. However, the sample P01 and P99 are 132°C and 245°C, and the P10/P90 ratio drops slightly to 1.45. An even more extreme truncation is possible by mapping the low and high inputs to the P01 and P99 percentile values. Sampling this distribution leads to Figure 2E, where the P10, P50, and P90 values are 160°C, 177°C, and 196°C, with a P10/P90 ratio of 1.23, similar to the triangular distribution.
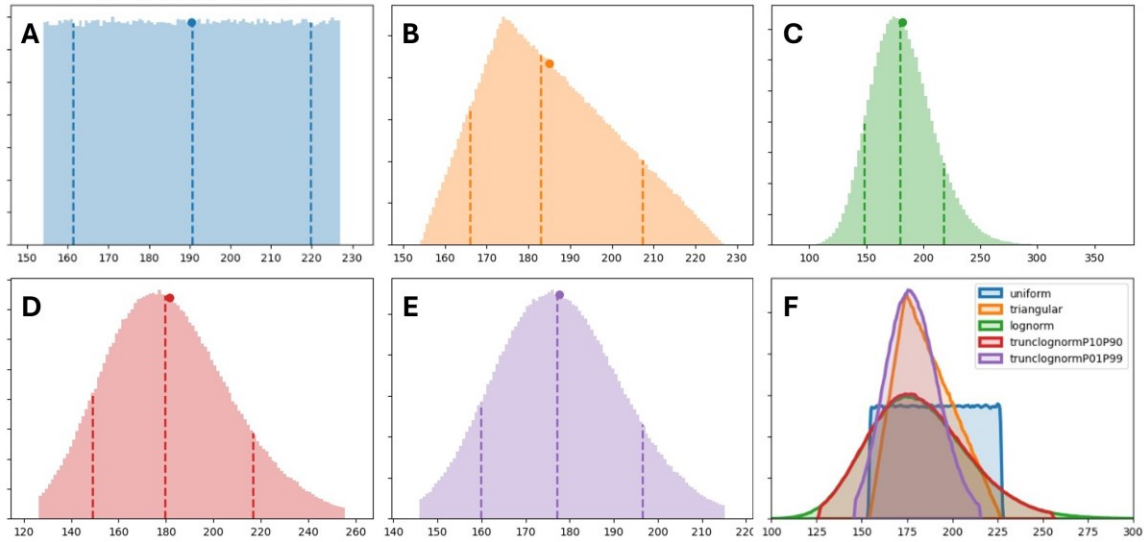

Figure 2: A.-E. Histograms generated from random-sampling distributions of the Silver Peak reservoir temperature values (low, mid, high = 154°C, 174°C, 227°C) 1 million times and visualizing with 100 bins. Plots are normalized such that the total area in each histogram equals 1. Vertical dashed lines indicate the P10, P50, and P90 locations in the distribution. The circle marker illustrates the mean. Distribution choices include A. uniform, B. triangular, C. lognormal, D. lognormal with low and high inputs treated as P10 and P90 locations, then truncated at P01 and P99, E. lognormal with low and high inputs treated as P01 and P99 locations, then truncated at P01 and P99. F. Overlay of KDE representations of the sample distributions to show relative proportions and breadth.

Figure 2F displays all five distributions simultaneously to visualize the assumptions inherent in each distribution choice. Uniform distributions assert certainty only in the extremes, with no clear central value bias. This would be appropriate if the only information available is the absolute endmembers of a variable's possible value. Triangular distributions fully adhere to the inputs, setting hard cut-offs at the low and high values, while setting the mode to the user-defined middle value. As a distribution choice, this allows for a stronger focus of the preconceived value for the variable, while also disallowing values outside of the low/high range to ever appear. For exploration, choosing this distribution would be appropriate if you have some data (e.g., from geothermometry) and know high/low values that define true boundaries of what might be possible in the subsurface. Lognormal distributions accept a greater amount of uncertainty by allowing higher and lower values than the other distributions. Without constraints, the low and high reservoir temperatures observed from random sampling are 89°C and 382°C (Figure 2C). Naturally, this allows for the real-world variation in subsurface properties to be imagined in a sample-based estimation technique like Monte Carlo. Truncation constraints like in Figure 2D can rein in the range such that the low/high values observed are 126°C and 255°C, however tightening the constraints further only serves to mold the lognormal into a pseudo-triangular distribution with the P50 as the mode. One danger of manipulating the distribution to this degree is demonstrated in Figure 2F (purple curve); while the P90/P10 ratio matches that of the triangular (orange curve), the lognormal is left-shifted in comparison and does not encompass the high value used as an input parameter for constructing the distribution (227°C).

3.3 Input Variable Sensitivities
Before detailing how to appropriately apply distributions to inputs for the HIP method, it is useful to identify which variables have the greatest influence on the resource estimate. This understanding helps prioritize efforts and refine focus on the most impactful variables.

Figure 3 illustrates a tornado diagram of the different possible inputs based on the 1975 formulation (Equations 1-2), extended to include variables used for the three-component reservoir characterization (i.e., Equation 5). The sensitivity test starts with defining the extremal values for each variable. Unless otherwise specified, the values used correspond with those described in Circular 790 (Brook et al., 1979). For Area, we chose a low value of 0.75 km^2 – the size based on a 500 m radius around a single vertical well – and capped the high value at 10 km^2. Some fields have reservoir areas significantly larger than this, e.g., 70+ km^2 for The Geysers (Renner et al., 1975), but the overwhelming influence of Area on the plot required a more conservative high end. For reservoir thickness, we chose 500 m as an EGS-centric low value. Volumetric specific heat values are derived from a wide range of thermal conditions reported by Vosteen and Schellschmidt (2003). Porosity assumes a low of 0%, 5% most common (Figure 4, Ciriaco et al., 2020), and a high of 15% as seen in Darajat field (Rejeki, 2001). The reservoir temperature range is consistent with binary through double flash systems around the world. Reference temperatures cover the triple point of water, the typical condenser temperature, and the highest value noted by Ciriaco et al. (Fig. 5, 2020). For recovery factor and conversion efficiency, we used the references in Table 1 to set the ranges. Plant capacity factor and field life values align with literature and published summaries (Ciriaco et al., 2020).

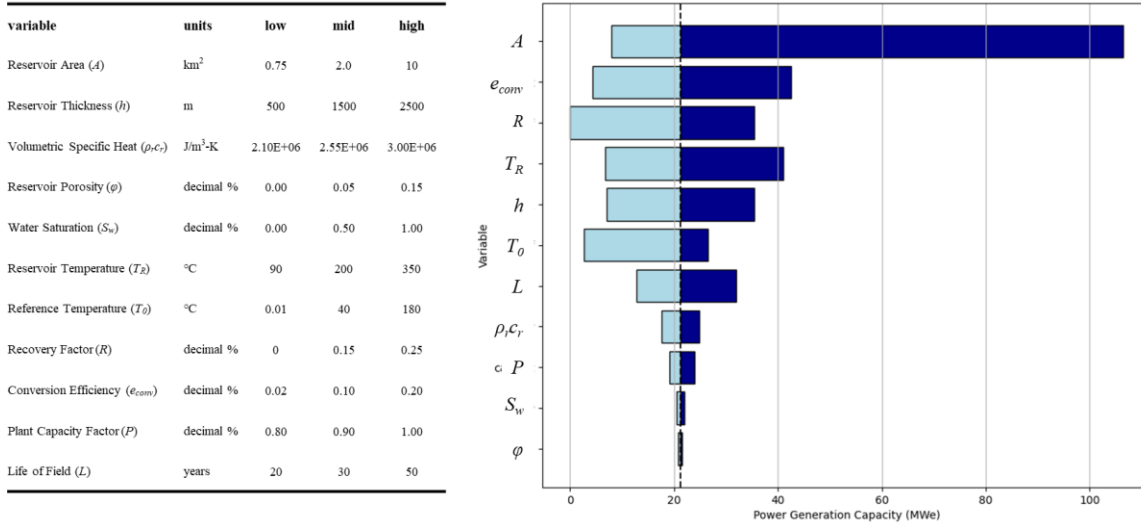| variable	units	low	mid	high
Reservoir Area (A)	km^2	0.75	2.0	10
Reservoir Thickness (h)	m	500	1500	2500
Volumetric Specific Heat ($\rho_r c_r$)	J/m^3-K	2.10E+06	2.55E+06	3.00E+06
Reservoir Porosity (φ)	decimal %	0.00	0.05	0.15
Water Saturation (S_w)	decimal %	0.00	0.50	1.00
Reservoir Temperature (T_R)	°C	90	200	350
Reference Temperature (T_0)	°C	0.01	40	180
Recovery Factor (R)	decimal %	0	0.15	0.25
Conversion Efficiency (e_{conv})	decimal %	0.02	0.10	0.20
Plant Capacity Factor (P)	decimal %	0.80	0.90	1.00
Life of Field (L)	years	20	30	50

Figure 3: Sensitivity testing of the USGS method. The vertical dashed line shows results when middle values are used for each variable, while horizontal bars show the range of outcomes as the respective variable's low/high values are applied. Variables are sorted to show the most influential at the top. Each input variable's range was based on resource estimation literature or real-world examples. For visualization purposes, the high-side area is restricted to 10 km², even though some fields exceed this size.

Volumetric methods are highly sensitive to the reservoir volume, which is dominated by the Area factor. Ensuring inputs for reservoir area are well-characterized for most likely value as well as high and low extremes will strongly influence the quality of the estimate in early exploration. Somewhat surprisingly, the efficiency factor comes in second, nearly tied with recovery factor. Both variables play a significant role in the resource assessment and must be appropriately tuned to the type of geothermal system (hydrothermal vs. EGS) and the class of geothermal opportunity (e.g., lower enthalpy/binary plant or higher enthalpy/flash plant). Reservoir temperature and thickness round out the top 5 most influential variables. These variables warrant refined focus, as does the consistent choice of reference temperature and field lifespan. The remaining variables have a minor effect on the power estimate outcome.

3.4 Input Variable Constraints

3.4.1. Reservoir Area

As the most impactful input variable, close attention should be paid to defining both the high side potential and low side outcomes for the reservoir extent. A lognormal distribution is recommended to help counter certainty bias and consider a broader range of potential realities. We recommend a truncated lognormal constructed by setting the initial P10 and P90 to the estimated low and high values for reservoir area. However, visualize the distribution and check the extremes – area shouldn't be so small as to not reflect a single well development nor so large as to be geologically infeasible given available subsurface data.

Another factor to keep in mind is accessibility of the surface rights and the likely scale of development. In national estimates of geothermal potential, these constraints may not come into play. However, consider an EGS opportunity targeting a deep formation covering 10's to 100's of squared kilometers; this will not be developed in a single project. Ensure the high-side areal extent is achievable and truly representative of the scale of assessment being undertaken, be it regional or individual project-scale.

3.4.2. Reservoir Thickness

The HIP method views a geothermal reservoir as a block of uniform thickness. The range of values for this variable should therefore be treated as uncertainty in the average value over the full reservoir area rather than applying the limits of local thickness variations. Use a uniform distribution for h if hard bounds are justified, and if the most likely value is found through subsurface evaluation, use a triangular distribution instead. Otherwise, a truncated lognormal may be most appropriate, but visualize the distribution to ensure the shape and endpoints are geologically reasonable. Also, consider deviated drilling when defining A and h, especially in EGS developments where horizontal wells can cover large map extents but provide limited vertical access to the reservoir.

3.4.3. Reservoir Temperature

Reservoir temperature should also represent an average across the full reservoir volume. As a natural property of the subsurface, we recommend using a lognormal distribution constructed from geothermometry, well surveys, or analog data given the uncertainties inherent in those methods. Visualization of the distribution is highly recommended and use of a truncated lognormal if unreasonably high or low extreme reservoir temperatures could be selected from random sampling.

3.4.4. Recovery Factor

Among the different input variables to the HIP method, recovery factor (R) has uniquely driven significant debate among researchers. Initial recovery factors of around 25% (Nathenson & Muffler, 1975; Muffler & Cataldi, 1978; Brook et al., 1979) were poorly constrained, relying on idealized models and the assumption that geothermal systems behave like Lardarello or The Geysers. Non-ideal reservoir behavior was even assumed to reduce the recovery factor by one-half. One point of consensus was the need for calibration through field studies (e.g., Nathenson, 1975; Muffler & Cataldi, 1978), which took about two decades. Sanyal et al. (2002, 2004) compared past stored-heat assessments with actual power plant performance and numerical simulations, concluding 25% to be an overestimate. Other studies have supported this conclusion (Williams, 2004, 2008; Grant, 2014, 2018).

For general purpose application, the range proposed by Sanyal et al. (2004) of 3-17%, with a most likely of 11%, captures low outcomes of fracture-dominated systems (including EGS), allows for higher recovery sedimentary reservoir scenarios, and roughly aligns with ranges described by others (e g., Quinao & Zarrouk, 2014; Garg & Combs, 2015; Takahashi & Yoshida, 2018). Noting the relationship between recovery factor and reservoir reference temperature, we suggest using 3-15%, with a most likely at 10%, when T_0 is assigned to ambient conditions (e.g., 15°C). If T_0 uses abandonment temperature, we suggest 5%-20%, with a most likely at 13%. Furthermore, we recommend a truncated lognormal distribution for recovery factor to allow for rare cases outside of these bounds. In the case where T_0 is set to abandonment temperature, this distribution has a mean of 11%, minimum of 3%, maximum of 34%, and P90/P10 of 3.8.

3.4.5. Conversion Efficiency

Studies of the conversion efficiency in global geothermal fields have produced several relationships linking reservoir temperature or enthalpy with efficiency for use in modeling (e.g., Zarrouk and Moon, 2014; Ciriaco et al., 2020). Applying these relationships simplifies a resource estimate by explicitly linking one random variable (T_R) with another (e_{conv}) where the dependency between the two is already known to exist. Here, again, we refer to whole system conversion efficiency, which accounts for subsurface, production, and power cycle elements that may impact the translation of thermal energy in the reservoir into electrical power in the plant. Individual power plant components like turbines and generators can have very high efficiency values, but those are sub-efficiencies that multiply against factors linked to other system elements like friction within the wellbore, separation losses in two-phase systems, non-condensable gas presence, equipment heat losses, and auxiliary power consumption (Zarrouk and Moon, 2014). We recommend using the general efficiency function from Ciriaco et al. (2020) to perform lookups during Monte Carlo simulation:

$$e_{conv} = 7.6301 \ln(h_{wR}) - 43.9589, \tag{6}$$

where h_{wR} is enthalpy of the reservoir, proxied by the enthalpy of liquid water at reservoir temperature. Alternatively, use a triangular distribution that captures the range of efficiencies for the expected reservoir temperature range based on Figure 8 in Ciriaco et al. (2020).

3.4.6. Other Variables

The reservoir reference temperature (T_0) serves as a baseline for recoverable stored heat and thus should be treated as a constant that pairs with the choice of recovery factor. For the conservative R range, setting T_0 to a low value like 0.01°C (triple point of water) or 15°C (average surface temperature in the U.S.) would be acceptable. The choice between these two equates to roughly 5% difference in the final estimate, which can be considered minor given the uncertainties involved in early exploration assessments. For the higher range of R values, we suggest matching T_0 with the abandonment temperature for binary cycle (usually 100-110°C) or flash plants (usually 150-180°C). Being overly precise is misaligned with the uncertainties in greenfield exploration, so we recommend using 100°C when reservoir temperature (T_R) is expected to support binary cycle operations and 175°C otherwise.

Resource estimates show sensitivity to field life (L), although standard practice sets this variable to a constant. We recommend the same convention used by the original USGS Circulars of 30 years, which matches most other resource assessments.

Reservoir volumetric specific heat ($\rho_r c_r$) follows a relatively narrow range and, given its lower influence on the overall estimate, can be treated as a constant value of 2700 kJ/m^3 K to align with the original USGS Circulars for simplicity.

The plant capacity factor (P) for geothermal power plants is typically quite high. Standard practice employs values $\geq 90\%$ for assessments. Older power plants experience more down-time; however, since this variable is not highly impactful, it is advisable to apply a constant value between 90-95%. We will use 95% in the next section.

Both porosity (φ) and water saturation (Sw) only matter if the resource assessment accounts for fluid and steam in the pore space of the reservoir. As noted earlier, stored heat from water components tends to be 10% or less of the total reservoir thermal energy. For greenfield exploration, where the determination of porosity and water saturation is not yet well constrained, we recommend using Equation 1 for the whole reservoir and exclude both φ and Sw from the calculation.

3.5 Bias Checking

Once distributions have been assigned to all input variables, generating a probabilistic resource estimate is simply a matter of random sampling the distributions and applying HIP calculations in a Monte Carlo simulation. Figure 4 illustrates results after simulating 100,000 scenarios for the Soultz-sous-Forêts EGS example in Table 2, using P10/P90 truncated lognormal distributions for inputs except for constants applied to $\rho_r c_r$, T_R, P, and L as discussed above. We applied Equations 1-2, representing reservoir without splitting out water and steam components. The conversion efficiency was calculated for each scenario using Equation 6 with enthalpy values based on sampled reservoir temperatures. Electrical power generation capacity is plotted as a cumulative distribution function or "S-curve," with the P10, P50, and P90 estimates highlighted. Note the long tail on the high side, indicating the outcome is lognormal-distributed and, in rare cases, realizes values of more than 30 MWe (P99.9). More generally, the outcomes are in the single digits, and the smallest scenario totaling just 200 kWe. For comparison, the current installed capacity of the actual Soultz power plant is 1.7 MWe, which lands on this distribution at the P22 value (Mouchot et al., 2018).
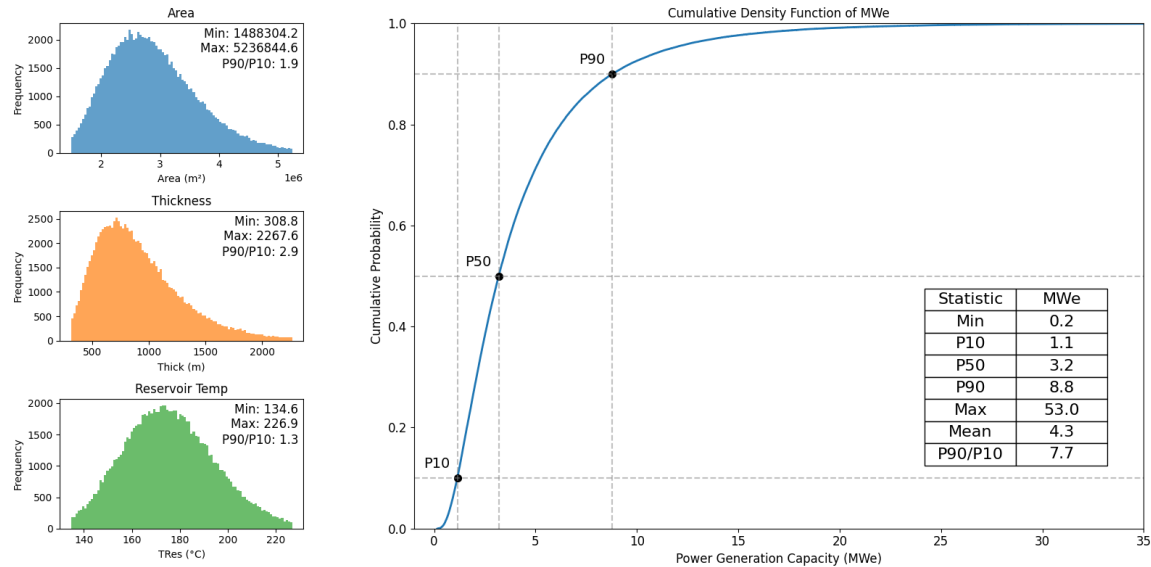

Figure 4: Example results view for a probabilistic HIP resource assessment using the Soultz-sous-Forêts example from Table 2. Left: Histograms display 100,000 random samples against distributions for reservoir area, thickness, and temperature. Annotations note the minimum and maximum value observed and the distribution P90/P10 ratio. Right: Predicted power generation capacity is displayed as a cumulative distribution function. The P10/P50/P90 values are highlighted and included in the inset table along with minimum, maximum, and mean results from the simulation. Also in the table is the P90/P10 ratio, which can indicate when estimates are over-confident for an exploration prospect.

The earlier discussion about bias is relevant here. In oil & gas exploration, addressing an explorer's certainty bias begins with verifying whether the lower end of the distribution aligns with a single well development case (Rose et al., 2004). It is important to note that including power predictions at or below zero MWe is not the intended goal. All results in the distribution should represent a success case outcome (technical or commercial), while failure should be separately assessed through a risk evaluation. Instead, ensuring that a low productivity success case is represented in the distribution, as it is in this instance, serves as a measure against over-optimism.

Next, a close inspection of the P90/P10 ratio can highlight whether the range of predicted outcomes is too narrow. Experts have debated whether there are "correct" P90/P10 ratios for different project stages, e.g., oil and gas professionals in the 1980s and 1990s suggested ratios should range from $\approx$ 2-7 for development wells, 5-25 for step-out extensions, and 10-100s for wildcat exploration wells (see Table 6 in Rose, 2001). Studies on exploration portfolio management practices have led some to argue the appropriate ranges will vary for each company and require look-back calibration (Otis and Haryott, 2006). In the example illustrated, a P90/P10 of 7.7 might indicate a slight degree of excess certainty if this opportunity was truly a greenfield EGS prospect. Both Area and Reservoir Temperature have low distribution P90/P10 ratios at under 2.0 (Figure 4, left inset plots). A good next step might be to review analogs and field data to see if these distributions could be widened a bit more. Data acquisition, rigorous analysis, and detailed reservoir modeling will naturally refine and narrow resource estimates for a prospect, so it is important to avoid excessive precision before the opportunity has been fully matured.

CONCLUSIONS

Early geothermal exploration evaluations of recoverable resources often use the USGS Volumetric Heat-in-Place (HIP) methodology, which can appear deceptively simple to apply at first glance. Reviewing equations from USGS Circulars and other sources highlights the potential complexity in characterizing the reservoir, estimating electrical power generation capacity, and choosing appropriate reference temperatures, efficiency factors, and recovery factors for probabilistic simulation. This study encourages an informed explorer's mindset, achieved by selecting the HIP derivation that keeps precision of reservoir and power cycle elements fit for purpose. It also involves carefully considering the distributions applied to each input variable, acknowledging the relationships between different inputs during value selection, and checking natural biases through visualizing and statistically assessing the shape of results distributions. The view of exploration opportunities will naturally change as they evolve in maturity from concepts to prospects, just as they refine during active project execution. Using additional data and rigorous modeling can narrow expected outcomes, making early bias mitigation crucial. Tracking historical estimates against outcomes helps test and recalibrate for bias, improving portfolio management through performance reviews. Future work will integrate lessons from these approaches to ensure consistent and accurate geothermal resource assessments, supporting a healthy and competitive geothermal business.

REFERENCES

Australian Geothermal Energy Association (AGEA). (2010). The Geothermal Reporting Code. In: The Australian Code for Reporting of Exploration Results, Geothermal Resources and Geothermal Reserves. 2nd edition, pp.34.

Brook, C. A., Mariner, R. H., Mabey, D. R., Swanson, J. R., Guffanti, M., & Muffler, L. J. P. (1979). Hydrothermal convection systems with reservoir temperatures> 90 C. Assessment of geothermal resources of the United States-1978: US Geological Survey Circular, 790, 18-85.

Ciriaco, A. E., Zarrouk, S. J., & Zakeri, G. (2020). Geothermal resource and reserve assessment methodology: Overview, analysis and future directions. Renewable and Sustainable Energy Reviews, 119, 109515.

Garg, S. K., & Combs, J. (2010, February). Appropriate use of USGS volumetric "heat in place" method and Monte Carlo calculations. In Proceedings 34th Workshop on Geothermal Reservoir Engineering, Stanford university, Stanford, California, USA.

Garg, S. K., & Combs, J. (2015). A reformulation of USGS volumetric "heat in place" resource estimation method. Geothermics, 55, 150-158.

GeothermEx. (2004) "New geothermal site identification and qualification. Final report.", April. https://doi.org/10.2172/897111.

Grant, M. A. (2014). Stored-heat assessments: a review in the light of field experience. Geothermal Energy Science, 2(1), 49-54.

Grant, M. A. (2018). Stored heat and recovery factor reviewed. In Proceedings: 43r d Workshop on Geothermal Reservoir Engineering. Stanford University, Stanford, California (pp. 1-8).

Hackstein, F. V., & Madlener, R. (2021). Sustainable operation of geothermal power plants: why economics matters. Geothermal Energy, 9, 1-30.

Mouchot, J., Genter, A., Cuenot, N., Scheiber, J., Seibel, O., Bosia, C., ... & Cuenot, N. (2018, February). First year of operation from EGS geothermal plants in Alsace, France: scaling issues. In Proceedings of the 43rd Workshop on Geothermal Reservoir Engineering, Stanford University, Stanford, CA, USA (Vol. 12).

Muffler, P., & Cataldi, R. (1978). Methods for regional assessment of geothermal resources. Geothermics, 7(2-4), 53-89.

Nathenson, M., & Muffler, L. J. P. (1975). Geothermal resources in hydrothermal convection systems and conduction-dominated areas. Assessment of geothermal resources of the United States-1975: US Geological Survey Circular, 726, 104-121.

Otis, R., & Haryott, P. (2006). How low should you go: a method to calibrate estimates of P99 prospect reserves. AAPG Convention. Houston, Texas.

Otis, R., & Haryott, P. (2010). Calibration of uncertainty (P10/P90) in exploration prospects. New Orleans: AAPG Convention.

Quinao, J. J., & Zarrouk, S. J. (2014, November). A Review of the Volumetric Stored-Heat Resource Assessment: One Method, Different Result. In Proceedings of 36th New Zealand Geothermal Workshop (pp. 24-26).

Rejeki, S. (2001). Reservoir porosity analysis at the Darajat Geothermal Field. In Proceedings.

Renner, J. L., White, D. E., & Williams, D. L. (1975). Hydrothermal convection systems. Assessment of geothermal resources of the United States, 7261975.

Rose, P. (2001). AAPG Methods in Exploration No. 12, Chapter 3: Risk Analysis of Exploration Prospects.

Rose, P.R. (2004). Chronic Exploration and Production Under-Performance: Is Dennis Horner's "Inevitable Disappointment" Portfolio Model Really Inevitable? AAPG International Conference: October 24-27; Cancun, Mexico.

Sanyal, S. K., & Sarmiento, Z. (2005). Booking geothermal energy reserves. Geothermal Resources Council Transactions, 29, 467-474.

Sarmiento, Z. F., Steingrímsson, B., & Axelsson, G. (2013). Volumetric resource assessment. Proceedings of the Short Course V on Conceptual Modelling of Geothermal Systems, Santa Tecla, El Salvador, 2.

Sugino, H., & Akeno, T. (2010, April). 2010 country update for Japan. In Proceedings World Geothermal Congress.

Takahashi, S., & Yoshida, S. (2018). A desktop review of calculation equations for geothermal volumetric assessment. 43Workshop on Geothermal Reservoir Engineering, 18-18.

Tester, J. W., Anderson, B. J., Batchelor, A. S., Blackwell, D. D., DiPippo, R., Drake, E. M., ... & Petty, S. (2006). The future of geothermal energy. Massachusetts Institute of Technology, 358, 1-3.

Vosteen, H. D., & Schellschmidt, R. (2003). Influence of temperature on thermal conductivity, thermal capacity and thermal diffusivity for different types of rock. Physics and Chemistry of the Earth, Parts a/b/c, 28(9-11), 499-509.

White, D. E., & Williams, D. L. (1975). Assessment of geothermal resources of the United States, 1975 (No. 726-730). US Department of the Interior, Geological Survey.

Williams, C. F., Reed, M., & Mariner, R. H. (2008). A Review of Methods Applied by the US Geological Survey in the Assessment if Identified Geothermal Resources (p. 27). US Department of Interior, US Geological Survey.

Wilmarth, M., Stimac, J., & Ganefianto, G. (2021, May). Power density in geothermal fields, 2020 update. In Proceedings World Geothermal Congress 2020 (Vol. 1, pp. 1-8).

Zarrouk, S. J., & Simiyu, F. (2013, November). A review of geothermal resource estimation methodology. In Proceedings, New Zealand Geothermal Workshop, Rotorua.

Zarrouk, S. J., & Moon, H. (2014). Efficiency of geothermal power plants: A worldwide review. Geothermics, 51, 142-153.